Experimental Study for Buckling and Postbuckling Behaviors of Composite Laminates with Multiple Delaminations

SHUN-FA HWANG* AND GUU-HUANN LIU
Department of Mechanical Engineering
National Yunlin University of Science & Technology
123 University Road, Sec. 3
Touliu, Taiwan 640, R. O. C.

ABSTRACT: The buckling and postbuckling behaviors of composite laminates with multiple delaminations under uniaxial compression are experimentally studied. The through-width multiple delaminations with triangular shape are used to simulate impact damage. A nonlinear buckling analysis from finite element method is also used to predict the buckling loads that are compared with experimental results. The critical delamination growth loads of multiple delaminations are obtained from postbuckling tests. The difference of single delamination and multiple delaminations on buckling behavior and postbuckling behavior is discussed. The results indicate that the buckling loads obtained by the nonlinear buckling analysis are in reasonable agreement with the experimental values. Experiments have proven that short delaminations distributed under the near-surface, long delamination have no effects on the buckling loads. The critical delamination growth loads of single-delamination specimens are much higher than those of multiple-delamination specimens, and the shape of the triangular multiple delaminations can affect the critical delamination growth loads.

KEY WORDS: multiple delaminations, buckling, postbuckling, delamination growth, finite element analysis.

INTRODUCTION

BECAUSE OF THEIR laminated structure, fiber-reinforced composites are susceptible to delamination caused by manufacturing defects, object impacts, or high stress concentrations from geometrical discontinuity. When a delaminated composite plate is subjected to uniaxial in-plane compression, local buckling of the delaminated region or mixed mode buckling, which is a combination of local and

*Author to whom correspondence should be addressed. E-mail: hwangsf@pine.yuntech.edu.tw

0731-6844/02/01 0333–17 $10.00/0 DOI: 10.1106/073168402026253

global buckling, may occur before global buckling, as shown in Figure 1. The delaminated composite plate, therefore, has a lower ability to resist compressive loads. The reduction in this ability is dependent on the shape, area, and position of the delamination. However, if the delamination does not grow, the buckling of the delaminated composite plate may not represent immediate failure. Experiments indicated that delamination growth always occurs after buckling. Even after buckling, the delaminated composite plate can still suffer increasing load until the delamination grows. In this case the critical delamination growth load represents the ability of the delaminated composite plate to resist compressive loads. Therefore, understanding the effect of delamination on buckling load and delamination growth is necessary to design correctly and to safely use fiber-reinforced composite materials.

The research on this subject in the literature is mostly focused on single-delamination composite laminates. This single delamination assumed to be near surface and through-width was treated as a thin film problem [1], one-dimensional model [2], or a sublaminate on an elastic foundation [3]. Advanced methods for determining buckling loads were also proposed, for example, continuous analysis [4], variational principle [5], the Rayleigh-Ritz method and finite element analysis [6,7]. The effects of transverse shear or higher order plate theory were evaluated by Chen [8] as well as Chattopadhyay and Gu [9]. The buckling of

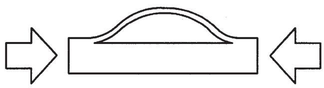

(a) Local buckling mode

(b) Mixed buckling mode

(c) Global buckling mode

Figure 1. *Three types of buckling mode shape.*

interply hybrid composites was studied analytically and experimentally [10] and the failures of delaminated composites under uniaxial compression were discussed by Hwang and Mao [11]. Besides the strip shape of delamination, a penny-shaped delamination [12] and an elliptic delamination [13–15] near the surface of composite laminates were also investigated.

Recently the problem of multiple delaminations attracts some attention because it's a better approximation of impact damage. The compressive buckling of composite panel with through-width, equal-size, equally-spaced multiple delaminations was investigated by Suemasu [16], with the Rayleigh-Ritz approximation technique and buckling testing conducted to verify the theoretical technique. Lee et al. [17] discussed the buckling of composite beam-plates with multiple delaminations by a finite element method based on a layer-wise plate theory and proved that short delaminations under the near-surface, long delamination have no effects on the buckling loads. The buckling of two close delaminations with unequal length was studied by Adan et al. [18] with a linear analysis. Kutlu and Chang [19] used a nonlinear finite element method and experiments to discuss the buckling and postbuckling behaviors of two far-away delaminations. Kyoung et al. [20] also applied a nonlinear finite element method to investigate the buckling and postbuckling of two delaminations or multiple delaminations with equal length. Huang and Kardomateas [21] used a nonlinear beam theory to predict the critical buckling loads of two delaminations with unequal length and concluded that if the longer delamination is outside of the shorter delamination, the latter has no effect on the buckling loads. Otherwise, the shorter delamination can reduce the buckling loads. Larsson [22] employed the von Karman plate theory to determine axisymmetric buckling and postbuckling behaviors of isotropic plates containing a multiple number of circular delaminations. The instability growth of multiple penny-shaped delaminations in circular axisymmetric plates subjected to a transverse concentrated load was discussed by Suemasu and Majima [23]. Suemasu et al. [24,25] used the Rayleigh-Ritz method and experiments to obtain the buckling loads of multiple circular delaminations in composite plates with two fixed edges and two simply supported edges and applied a finite element method to study their postbuckling behaviors.

From the above description, multiple delaminations were still limited to some ideal shapes and their critical buckling loads were mostly predicted by analytical methods. Very few used experiments to observe the buckling behavior and to obtain the buckling load. The postbuckling behavior and the critical delamination growth loads of multiple delaminations have seldom been studied by experiments. The purpose of this work is to observe the buckling and postbuckling behaviors of composite laminates with multiple delaminations under uniaxial compression. The shape of multiple delaminations used is related to impact damage. A nonlinear buckling analysis from the finite element method is also used to predict the buckling loads that are compared with experimental results. The critical delamination growth loads of multiple delaminations are obtained from postbuckling testing. The difference between single delamination and multiple delaminations on buckling behavior and postbuckling behavior is discussed.

EXPERIMENTAL DETAILS

HTA1200A/ACD8801 carbon/epoxy was used to make the delaminated composite laminates. The mechanical properties of this composite are listed in Table 1. The Young's modulus, shear modulus, and Poisson's ratio are denoted as E, G, and ν, respectively. The subscript 1 represents the fiber direction and 2 the direction transverse to the fiber. To fabricate the laminate, the bag molding process and a two-stage curing cycle were used. The delaminations were introduced by inserting a 50 μm polytetrafluoroethylene (PTFE) film during the stacking process. The buckling specimens were cut from the laminate having 16 unidirectional plies by a diamond saw. The gauge length of the buckling specimen, L, shown in Figure 2 was selected as 100 mm, the width W 20 mm, and the thickness H about 1.6 mm. The ratios of the longest delamination length to specimen gauge length, a/L, were selected as 0.3, 0.5, and 0.7. The position of the longest delamination along the thickness direction is denoted as t.

The delaminated composite specimens considered are shown in Figure 2. The single-delamination specimen, shown in Figure 2(a), is used to compare with the multiple-delamination specimen. The triangular four-delamination specimen shown in Figure 2(b) is considered to approximate the damage caused by low velocity impact [2,14,22]. These four delaminations are evenly distributed from the second interface to the middle interface. Therefore, each strip between two delaminations has two composite layers. The variation of the b value in Figure 2(b) is to create different deduction rates for inner delaminations. The b value was changed from 1 mm to 7 mm for all cases considered except for the case of a/L = 0.3. In this case the b value was varied only from 1 mm to 5 mm because for b =7 mm we cannot have four delaminations.

The uniaxial buckling and postbuckling testing was conducted in a Shimadzu AGS-500G universal testing machine with a recorder to plot the load-end shortening displacement curve. The crosshead rate for loading the specimen was 0.2 mm/min. Three identical specimens for each specimen design were tested to get an average buckling load. During the testing, the buckling mode shape was carefully

Table 1. Mechanical properties of carbon/epoxy composites.

	E_{11} (GPa)	E_{22} (GPa)	G_{12} (GPa)	ν_{12}	V_f
Carbon/epoxy	**140**	**10.1**	**6.4**	**0.23**	**0.6**

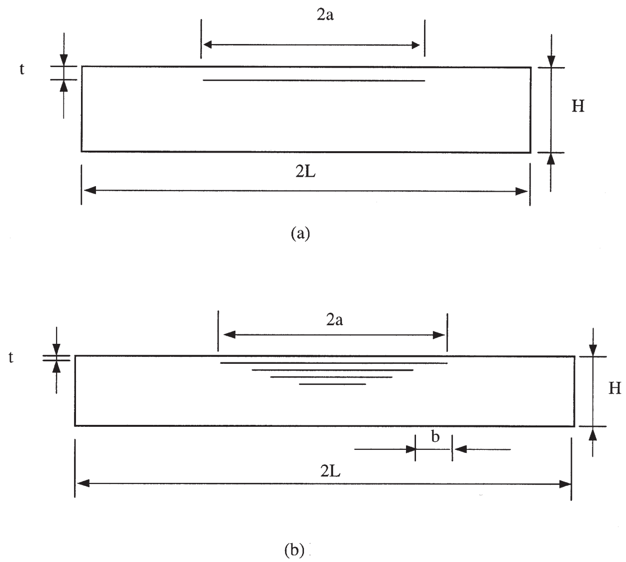

Figure 2. *Single-delamination and multiple-delamination specimens: (a) single-delamination specimen, (b) multiple-delamination specimen.*

observed and recorded. For the near-surface delamination, the buckling load is very low and cannot be determined from the load-end shortening displacement curve. Therefore, a strain gauge was mounted on the specimen surface that is close to the delaminated region. When the strain starts to increase from a negative value, as shown in Figure 3, buckling occurs and the corresponding buckling load is found. When this method is applied to the cases in which the buckling loads can be judged from the load-end shortening displacement curves, both results are very close [10]. Furthermore, it is found that the buckling loads of the three identical specimens are very close to each other. After buckling, the compressive displacement continues to increase until the delamination grows. During the testing, the configuration of the specimen at different loading stages is recorded by a digital camera. The critical load of delamination growth could be judged from the point in the load-end shortening displacement curve where the load dramatically decreases from its maximum.

NONLINEAR BUCKLING ANALYSES

Nonlinear buckling analysis and linear (or eigenvalue) buckling analysis are two techniques available in the finite element program for predicting the buckling load and buckling mode shape of a structure. The theoretical buckling load, based

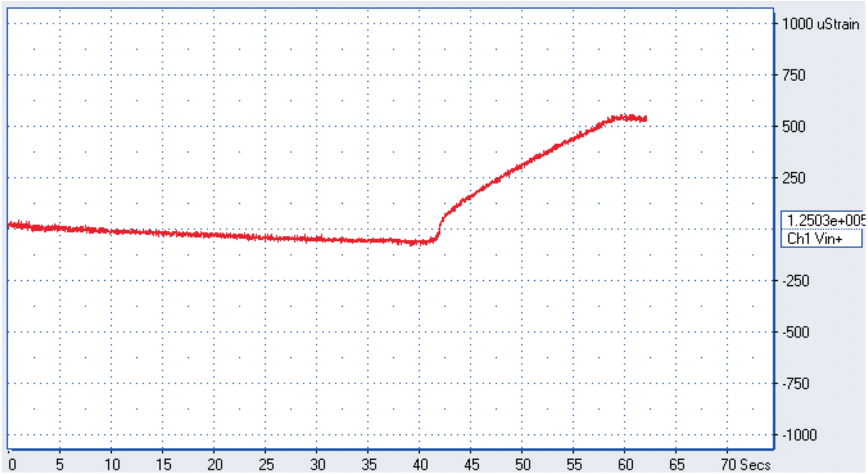

Figure 3. *Strain-elapsed time curve for buckling test.*

on linear buckling analysis, generally occurs at a point where the total stiffness of an ideal linear elastic structure vanishes. The total stiffness can be written in matrix form as

$$[K]_T = [K] + \lambda[S] \tag{1}$$

where $[K]$ is the linear stiffness matrix, $[S]$ the stiffness matrix from the effect of compressive load, and λ the scaling factor or eigenvalue. The structure buckles and $[K]_T = 0$, when the softening effect from the compressive loading overpowers the inherent structure stiffness such that no net stiffness remains and displacements increase without bound. The buckling load is determined by solving for eigenvalues and the corresponding eigenvectors represent the buckled mode shape. Due to imperfections and nonlinearities in most real-word structures, linear buckling analysis generally yields unconservative results.

A nonlinear buckling analysis is simply a nonlinear static analysis with gradually increasing the applied load to seek the load level at which the solution begins to diverge and the structure becomes unstable. Because some features such as initial imperfections and large-deflection response can be included, nonlinear buckling analysis is usually the more accurate approach and will be used in this work.

Using the material properties listed in Table 1, the commercially available finite element code ANSYS 5.3 is applied to calculate the buckling load. A half of the specimen is considered in the finite element analysis such that the three possible buckling modes are included. Two-dimensional quadratic eight-node plane strain elements are used to mesh the whole domain, except the crack tip region, which was meshed by singular elements to describe the singularity behavior and to reduce computational time. Contact elements are also used on the delamination surfaces to prevent the overlapping situations. The external load is applied on a very rigid block attached to the end of the structure to simulate the displacement-controlled boundary conditions in the experiments. There are about 919 to 1268 elements and 2091 to 3435 nodes for the different specimens.

An initial small geometric imperfection, which is necessary for initiating a nonlinear buckling analysis, is provided from the mode shape of linear buckling analysis. During each load increment the stiffness matrix must be adjusted to reflect the nonlinear changes in the structure stiffness, otherwise errors will accumulate. This difficulty is overcome using the Newton-Raphson equilibrium iterations, which drive the solution to convergence at the end of each load increment. It is also important to recognize that an unconverged solution does not necessarily mean that the structure has reached its maximum load. It could be caused by numerical instability. Tracking the load-deflection history of the structure can help to decide if the buckling occurs.

RESULTS AND DISCUSSION

Verification of Nonlinear Buckling Analysis

Nonlinear bucking analysis was used to predict the buckling loads of graphite/epoxy composite plates with single delamination and compared with experiments. Details of the comparison can be seen in Hwang and Mao [10]. They showed that the results obtained from nonlinear buckling analysis differ from the experimental values by less than 5%. For multiple delaminations, Lee et al. [17] applied a finite element method based on a layer-wise plate theory to predict the buckling loads of random short-fiber composites with equal-size multiple delaminations and verified their method with the experimental data from Wang et al. [6,7]. The comparison of the present nonlinear buckling analysis with Lee's method is shown in Figure 4. The results from both methods are almost identical. From the above comparison, the applicability of the present nonlinear buckling analysis is verified.

Buckling Behavior

Three curves of load-end shorting displacement as shown in Figure 5 are experimentally obtained from the multiple-delamination specimens with $a/L = 0.3$ and $b = 1$ mm, $a/L = 0.5$ and $b = 1$ mm, as well as $a/L = 0.7$ and $b = 7$ mm, respectively. The other cases with different delamination lengths and b values also have similar curves. The circles on these curves represent the points where a picture of the configuration was taken with a digital camera. Note again that the critical buck-

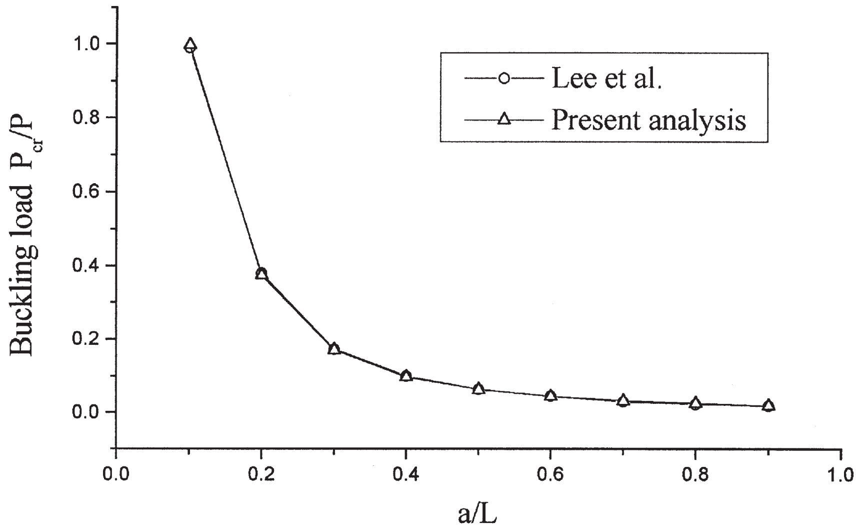

Figure 4. *Comparison of different analysis methods for predicting buckling loads.*

ling loads were determined with the aid of a strain gauge mounted on the specimen surface. However, for the cases of $a/L = 0.7$, the buckling loads could not be measured consistently by our system because of small values. This may be even worse due to the curved shape around the damaged region caused by the insert of the PTFE thin films. These results will not be discussed in the next section. But in these cases there is no problem for the critical delamination growth loads.

The buckling stresses of single-delamination and multiple-delamination specimens by both the nonlinear buckling analysis and the experiments are shown in Table 2 for $a/L = 0.3$ and Table 3 for $a/L = 0.5$. In these two tables the buckling stresses are obtained from buckling loads divided by the specimen cross section area. Each experimental data denotes an average value from three identical specimens and the maximum variation of buckling stresses among the three repeat tests is less than 4.4% for all the cases in Tables 2 and 3. Therefore, the repeatability of the buckling test is very good. The results from the nonlinear buckling analysis indicate that the single-delamination case and the multiple-delamination case have the same buckling stresses and the variation of the b value in the multiple-delamination specimens has no effects on the buckling stresses. Since in all cases the buckling is a local mode and only the outside strip above the longest delamination buckles, the influence of the inner, shorter delaminations can be neglected. The experimental results shown in Tables 2 and 3 also exhibit that the variation of the b value in the multiple-delamination specimens has no effects on the buckling stresses. However, comparing the experimental buckling stresses

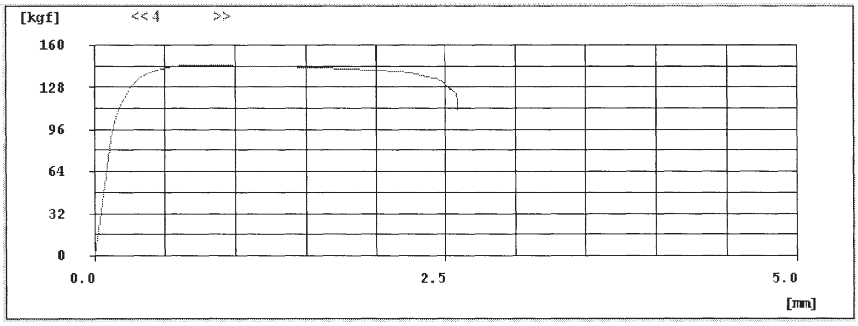

(a)

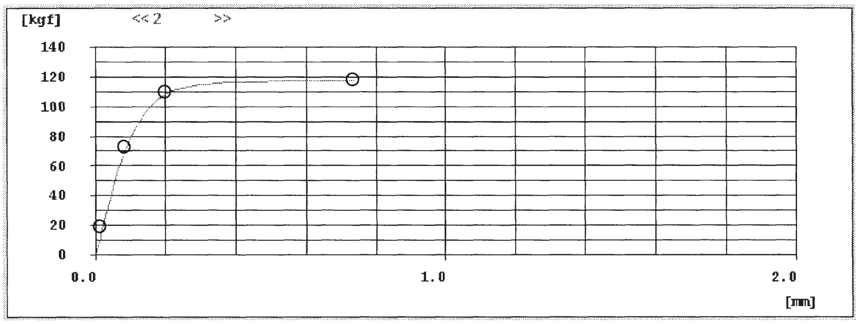

(b)

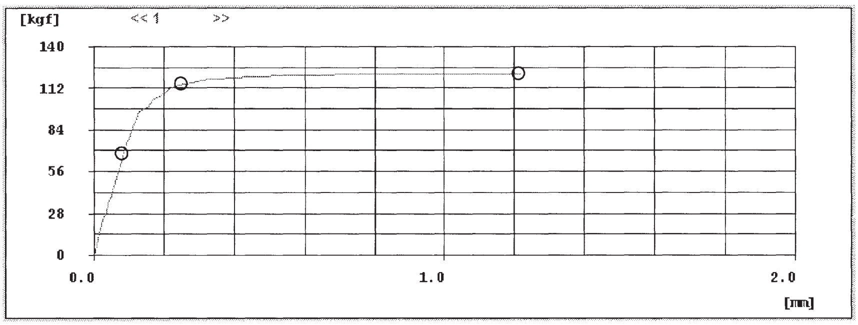

(c)

Figure 5. *Load-end shortening displacement of multiple delamination buckling: (a)* a/L = *0.3 and* b = *1 mm, (b)* a/L = *0.5 and* b = *1 mm, (c)* a/L = 0.7 and *b* = 7 mm.

Table 2. Buckling loads of specimens with a/L = 0.3.

	Single (GPa)	*b* = 1 mm (GPa)	*b* = 3 mm (GPa)	*b* = 5 mm (GPa)
Analysis	62.05	62.29	62.32	62.00
Experiment	53.93	47.10	45.67	46.77

between the single-delamination specimens and the multiple-delamination specimens, there is a 12% to 18% difference. This difference possibly comes from the curved shape around the delaminated region caused by the four PTFE inserts in the multiple-delamination specimens. It will make the specimens easier to buckle. From these two tables, one can see that the analysis results and the experimental values for the cases of $a/L = 0.5$ match very well, but not so well for $a/L = 0.3$. In addition to the curved shape caused by the insert thin films, the misalignment of specimens during the buckling test can explain some of these differences. This effect becomes more significant as the applied loads become larger.

Since the longest delamination is located at $t/H = 1/8$, a local buckling mode is observed from both the analysis and the experiments. As described above, from analysis this local buckling is only limited to the outer strip. This is also true for experimental cases. During the testing, one can observe the buckling of the outer strip quickly and sequentially followed by the buckling of the other inner strips. The buckling stresses measured are the critical values of the first buckling such that can be compared with the analysis data.

Experimental Postbuckling Behavior

After buckling the compressive displacement continues to increase until the delamination grows. As described above, the buckling of the inner strips quickly and sequentially occurs after the buckling of the outer strip. Then the buckling mode switches from a local one to a mixed one. When the delaminations become larger, for example $a/L = 0.7$, the mixed buckling mode becomes closer to a local symmetric buckling mode [17]. However, in our opinion, it is still a mixed mode. Figures 6–8 show the configurations of the specimens before and after the growth of the delamination. Right before delamination growth, when the *b* values are

Table 3. Buckling loads of specimens with a/L = 0.5.

	Single (GPa)	*b* = 1 mm (GPa)	*b* = 3 mm (GPa)	*b* = 5 mm (GPa)	*b* = 7 mm (GPa)
Analysis	22.70	22.17	22.12	21.20	22.01
Experiment	21.93	17.97	16.80	17.83	18.30

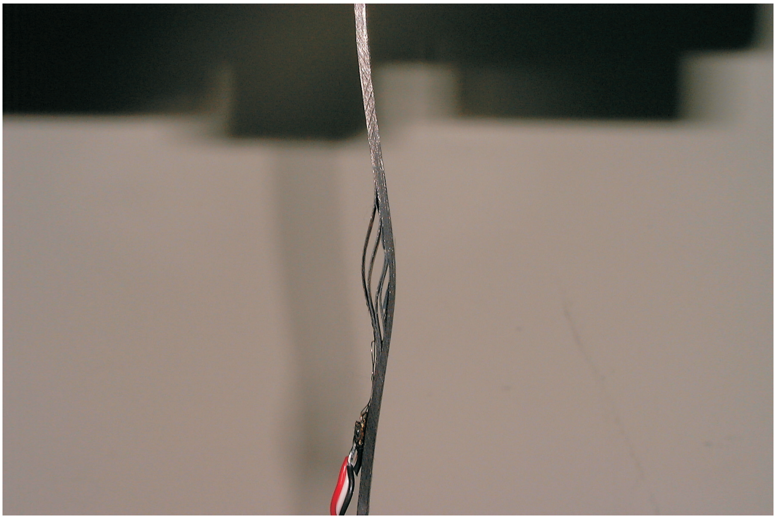

(a)

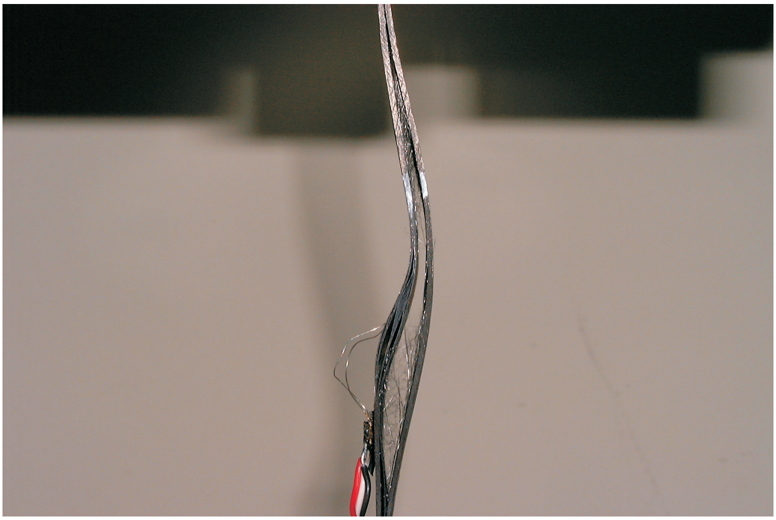

(b)

Figure 6. *Postbuckling behavior of multiple delamination specimens with* a/L = *0.3 and* b = *5 mm: (a) before delamination growth, (b) after delamination growth.*

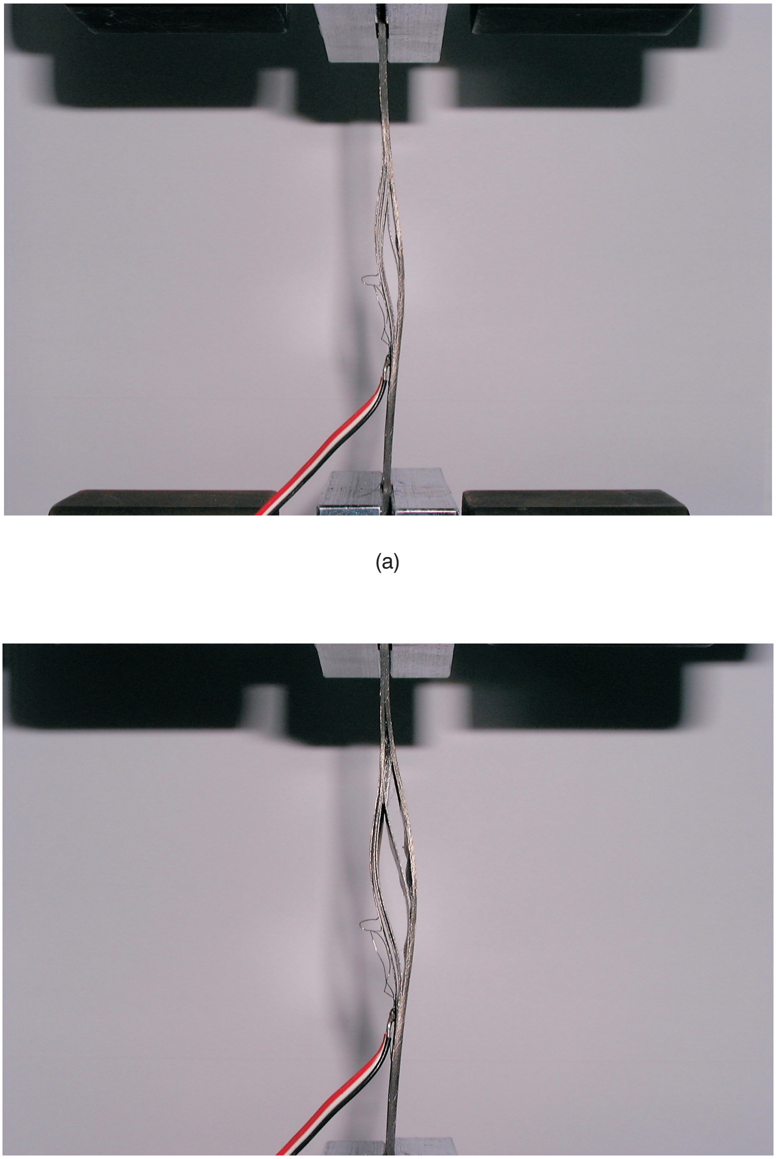

Figure 7. *Postbuckling behavior of multiple delamination specimens with* a/L = *0.5 and* b = *1 mm: (a) before delamination growth, (b) after delamination growth.*

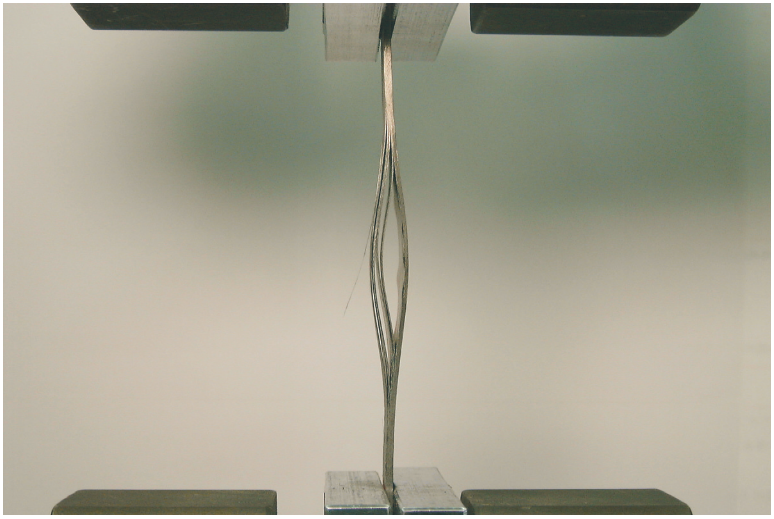

(a)

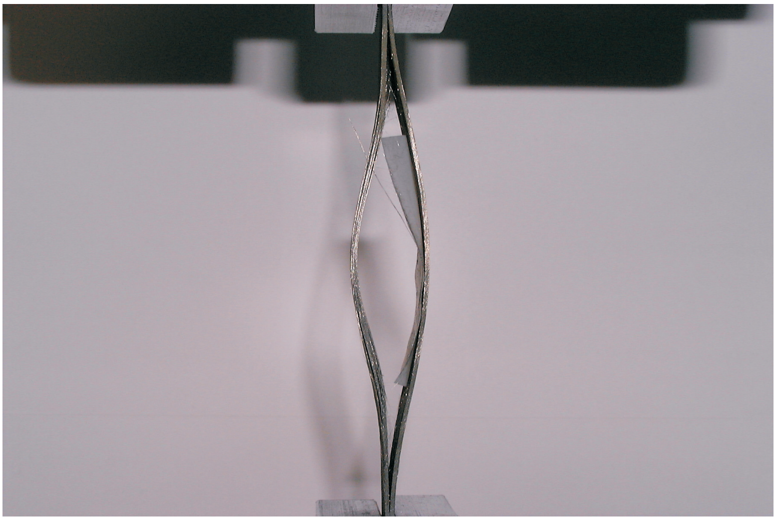

(b)

Figure 8. *Postbuckling behavior of multiple delamination specimens with* a/L = *0.7 and* b = *7 mm: (a) before delamination growth, (b) after delamination growth.*

larger such that the delaminations have very different lengths, all strips are clearly separated from one another without contact, as shown in Figures 6(a)–8(a). For the cases of small b values and similar delamination lengths, some strips are still close together after buckling. From Figures 6(b)–8(b), the interface of delamination growth for multiple-delamination specimen is totally different from that for single-delamination specimens, which is in the only delaminated interface [11]. For the cases of a/L = 0.3 and a/L = 0.7, the delamination growth of multiple-delamination specimens is along the inmost delaminated interface, which is also the middle interface. For the cases of a/L = 0.5, as shown in Figure 7(b), the upper part of the delaminations grows along the middle interface and the lower part grows along the third delaminated interface, which is the one next to the delaminated middle interface. From our information, it is difficult to tell which one goes first or simultaneously. After the delamination grows, the phenomenon of fiber bridging is pronounced as shown in these figures.

The critical loads of delamination growth can be determined from the point in the load-end shortening displacement curve where the load dramatically decreases from its maximum. Table 4 shows the critical delamination growth loads of the single-delamination and multiple-delamination specimens from the postbuckling tests. Each value in Table 4 is also an average from three identical tests and the maximum deviation of each test result from the average value is less than 5 %. The critical delamination growth loads of single-delamination specimens are two to three times larger than those of multiple-delamination specimens. This is different from the buckling loads, which have close values for both types of specimens. The reason causing this difference in delamination growth loads is that the single-delamination specimens have a different delamination growth path with the multiple-delamination specimens. For buckling loads, one can use single delamination to represent multiple delaminations if the longest delamination is the closest to the surface and the others are inner and shorter, as shown in Figure 2(b). However, if one approximates the critical delamination growth load of multiple delaminations by that of single delamination, one may overestimate the ability of composites to compressive loading and therefore obtain very unconservative results. Furthermore, the b value in the multiple-delamination specimen has a very clear effect on the critical delamination growth load. As the b value increases, the

Table 4. Experimental delamination growth loads.

a/L	Single (GPa)	b = 1 mm (GPa)	b = 3 mm (GPa)	b = 5 mm (GPa)	b = 7 mm (GPa)
0.3	256.42	131.93	138.47	180.84	
0.5	251.34	119.50	126.51	134.03	147.42
0.7	242.87	87.3	95.31	104.03	120.13

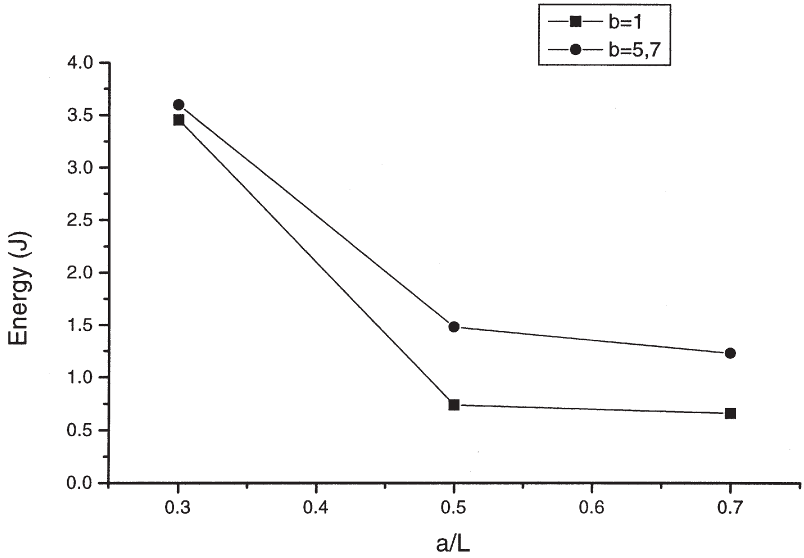

Figure 9. *Energy for delamination growth of multiple delamination specimens.*

critical delamination growth loads increase. This is because the specimens with higher b values have greater ability to resist further deformation during postbuckling. For the single-delamination case, the critical delamination growth load is only slightly decreased by the increase of a/L. For the multiple delamination case, this decrease is more evident.

If one uses the energy concept to represent the delamination growth, the results are shown in Figure 9. The energy in this figure is obtained from the area under the load-end shortening displacement curves shown in Figure 5. Hence, it denotes the amount of energy required for the delamination to grow. In this figure, the solid circle shows that $b = 5$ mm for the case of $a/L = 0.3$ and $b = 7$ mm for the other two cases. It is clear from this figure that there is a big drop in the energy from $a/L = 0.3$ to $a/L = 0.5$. But there is no great difference between $a/L = 0.5$ and $a/L = 0.7$. The effect of the b value is small for the case of $a/L = 0.3$ and becomes larger for the other two cases.

CONCLUSIONS

The buckling and postbuckling behaviors of composite laminates with multiple delaminations under uniaxial compression have been experimentally studied. A triangle shape of multiple delaminations was used to approximate impact damage and a nonlinear buckling analysis was used to predict its buckling loads. The critical delamination growth loads were also measured from the postbuckling testing. From the above results and discussion, the following conclusions can be made.

1. The critical buckling stresses obtained by the nonlinear buckling analysis and experiments are in reasonable agreement such that both methods are validated.
2. Present work provides experimental evidence that shorter delaminations under the longest delamination have no effect on the buckling loads. Both the single-delamination specimens and multiple-delamination specimens considered have similar buckling loads.
3. For the cases investigated, the buckling mode is a local one and the postbuckling is in a mixed mode. As the delaminations become longer in the multiple-delamination specimens, the mixed mode is close to a local symmetric mode.
4. For the critical delamination growth loads, the single-delamination specimens have much higher values than the multiple-delamination specimens considered because the delamination growths of both specimen types are along different delaminated interfaces.
5. The shape of the triangular multiple delaminations can also affect the critical delamination growth loads.
6. If energy concept is used to describe the delamination growth, the case of $a/L = 0.3$ has the highest energy and the cases of $a/L = 0.5$ and 0.7 consume a similar amount of energy.

ACKNOWLEDGEMENTS

The support from the National Science Council, R. O. C., through Grant NSC89-2212-E-224-012 at National Yunlin University of Science & Technology is gratefully acknowledged.

REFERENCES

1. Kachanov, L. M., 1976. “Separation of Composite Materials,” *Mekh. Polim.*, 5:918–922.
2. Chai, H., Babcock, C. D. and Knauss, W. G., 1981. “One Dimensional Modeling of Failure in Laminated Plates by Delamination Buckling,” *International Journal of Solids and Structures*, 17:1069–1083.
3. Vizzini, A. J. and Lagace, P. A., 1987. “The Buckling of a Delaminated Sublaminate on an Elastic Foundation,” *Journal of Composite Materials*, 21:1106–1117.
4. Wang, J. T.-S., Cheng, S. H. and Lin, C. C., 1995. “Local Buckling of Delaminated Beams and Plates Using Continuous Analysis,” *Journal of Composite Materials*, 29:1374–1402.
5. Kyoung, W. M. and Kim, C. G., 1995. “Delamination Buckling and Growth of Composite Laminated Plates with Transverse Shear Deformation,” *Journal of Composite Materials*, 29:2047–2068.
6. Wang, S. S., Zahlan, N. M. and Suemasu, H., 1985. “Compressive Stability of Delaminated Random Short-Fiber Composites, Part I—Modeling and Methods of Analysis,” *Journal of Composite Materials*, 19:296–316.

7. Wang, S. S., Zahlan, N. M. and Suemasu, H., 1985. "Compressive Stability of Delaminated Random Short-Fiber Composites, Part II—Experimental and Analytical Results," *Journal of Composite Materials*, 19:317–333.
8. Chen, H. P., 1993. "Transverse Shear Effects on Buckling and Postbuckling of Laminated and Delaminated Plates," *AIAA Journal*, 30:163–169.
9. Chattopadhyay, A. and Gu, H., 1994. "New Higher Order Plate Theory in Modeling Delamination Buckling of Composite Laminates," *AIAA Journal*, 32:1709–1716.
10. Hwang, S.-F. and Mao, C.-P., 2000, "The Delamination Buckling of Single-Fiber System and Interply Hybrid Composites," *Composite Structures*, 49: 183–190.
11. Hwang, S.-F. and Mao, C.-P., "Failure of Delaminated Carbon/Epoxy Composite Plates under Compression," *Journal of Composite Materials* (in press).
12. Bottega, W. J. and Maewal, A., 1983. "Delamination Buckling and Growth in Laminates", *Journal of Applied Mechanics*, 50:184–189.
13. Shivakumar, K. N. and Whitcomb, J. D., 1985. "Buckling of a Sublaminate in a Quasi-Isotropic Composite Laminate", *Journal of Composite Materials*, 19:2–18.
14. Chai, H. and Babcock, C. D., 1985. "Two-Dimensional Modeling of Compressive Failure in Delaminated Laminates", *Journal of Composite Materials*, 19:67–98.
15. Yeh, M. K. and Tan, C. M., 1994. "Buckling of Elliptically Delaminated Composite Plates", *Journal of Composite Materials*, 28:36–52.
16. Suemasu, H., 1993. "Effects of Multiple Delaminations on Compressive Buckling Behaviors of Composite Panels," *Journal of Composite Materials*, 27:1172–1192.
17. Lee, J., Gurdal, Z. and Griffin, O. H., Jr., 1993. "Layer-Wise Approach for the Bifurcation Problem in Laminated Composites with Delaminations," *AIAA Journal*, 31:331–338.
18. Adan, M., Sheinman, I. and Altus, E., 1994. "Buckling of Multiply Delaminated Beams," *Journal of Composite Materials*, 28:77–90.
19. Kutlu, Z. and Chang, F. K., 1992. "Modeling Compression Failure of Laminated Composites Containing Multiple Through-Width Delaminations," *Journal of Composite Materials*, 26:350–387.
20. Kyoung, W. M., Kim, C. G., Hong, C. S., and Jun, S. M., 1998. "Modeling of Composite Laminates with Multiple Delaminations under Compressive Loading," *Journal of Composite Materials*, 32:951–968.
21. Huang, H. and Kardomateas, G. A., 1998. "Buckling of Orthotropic Beam-Plates with Multiple Central Delaminations," *International Journal of Solids and Structures*, 35:1355–1362.
22. Larsson, P. L., 1991. "On Multiple Delamination Buckling and Growth in Composite Plates," *International Journal of Solids and Structures*, 27:1623–1637.
23. Suemasu, H. and Majima, O., 1996. "Multiple Delaminations and Their Severity in Circular Axisymmetric Plates Subjected to Transverse Loading," *Journal of Composite Materials*, 30:441–453.
24. Suemasu, H., Kumagai, T. and Gozu, K. 1998. "Compressive Behavior of Multiple Delaminated Composite Laminates Part 1: Experiment and Analytical Development," *AIAA Journal*, 36:1279–1285.
25. Suemasu, H., Kumagai, T. and Gozu, K. 1998. "Compressive Behavior of Multiple Delaminated Composite Laminates Part 2: Finite Element Analysis," *AIAA Journal*, 36:1286–1290.